Journal of the Brazilian Society of Mechanical Sciences and Engineering (2024) 46:399
https://doi.org/10.1007/s40430-024-04954-3

REVIEW PAPER

A comprehensive review of methodology and advancement in the development of superhydrophobic membranes for efficient oil–water separation

Avinash Kumar[1] · Vishal Mishra[1] · Yadav Narendra Kumar Rajbahadur[1] · Sushant Negi[1] · Simanchal Kar[1]

Received: 28 September 2023 / Accepted: 28 April 2024 / Published online: 28 May 2024

Abstract

Oil–water filtration is a highly challenging task and often faces difficulties like poor separation efficacy, high cost, and sometimes environmental impact like spreading microplastics from the mesh. The filtration processes are usually costly and primarily targeted to large-scale filtration. However, domestic wastes, industrial effluents, and construction site pollutants are often overlooked due to the unavailability of low-cost filters. Therefore, integrating additive manufacturing processes can significantly enhance oil–water separation. In this paper, it is observed from the review that 3D-printed separation devices exhibit enhanced performance and design flexibility. Further, in recent reports, 3D printing has been utilized to fabricate micro-scale and nano-scale structures on the surface with low surface energy. Tentatively, silane and chemical compounds like thiols, stearic, lauric, and oleic acids with extended functional groups are widely employed for surface modifications to enhance the performance of SHSO surface. With a high level of versatility in the 3D printing process, it is easier to develop tailored OWS solutions that address the unique challenges of industrial applications. This paper reviews recent advancements related to oil–water separation with keen consideration to additively manufactured devices, comparing them under a single domain. Furthermore, OWS mechanisms are summarized considering the effects of surface properties, such as surface energy and wetting angle. This review also discusses the effectiveness of various polymeric coatings on SHSO surfaces, comparing separation efficacy and flux rate with uncoated meshes.

Keywords Superhydrophobicity · Biodegradable · Oil–water separation · Additive manufacturing

Abbreviations

OWS	Oil–Water Separation
OWM	Oil–Water Mixture
SHSO	Superhydrophobic and Superoleophilic
WCA	Water Contact Angle
AM	Additive Manufacturing
USBM	U.S. Bureau of Mines
IAH	Amott-Harvey Index
PTFE	Polytetrafluoroethylene
PVAC	Polyvinyl Acetate
SDBS	Sodium Dodecyl Benzene Sulphonate
PPS	Polypropylene Sulphide
HDTMS	Hexadecyltrimethoxysilane
POSS	Polyhedral Oligomeric Silsesquioxane
SSM	Stainless-Steel Mesh
HMDS	Hexamethyldisilane
FDM	Fused Deposition Modelling
SLS	Selective Laser Sintering
ABS	Acrylonitrile Butadiene Styrene
PS	Polystyrene
PC	Polycarbonate
HDPE	High-Density Polyethylene
PLA	Polylactic Acid
PDMS	Polydimethylsiloxane
MEK	Methyl-Ethyl-Ketone
DIW	Direct Inkjet Writing
CA	Cellulose Acetate
PSU	Polysulfone

Technical Editor: Ahmad Arabkoohsar.

✉ Simanchal Kar
simanchal@mech.nits.ac.in

[1] Department of Mechanical Engineering, National Institute of Technology, Silchar, Assam 788010, India

1 Introduction

Water pollution has significant detrimental effects on both aquatic and terrestrial organisms. Marine systems, including rivers, lakes, and oceans, are vital in supporting human livelihoods by facilitating food chains and influencing weather patterns. Pollution in these water bodies can have severe consequences for various life forms. Recognizing the global importance of this issue, the United Nations has identified it as a priority objective. The UN urges nations to prioritize the preservation of clean environments by giving equal attention to conserve both land and water resources. This approach is crucial for ensuring the sustainability and well-being of ecosystems and human societies. Water pollution is caused by various factors, such as oil spills and the frequent release of industrial oily effluent [1, 2]. Notably, oil spills have resulted in significant adverse effects on marine life. For example, in 2010, the Gulf of Mexico experienced an inadvertent oil spill, releasing 134 million gallons of oil, which impacted around 2100 km of the American Gulf Coast from Texas to Florida. This incident was described as "the worst environmental disaster America has ever faced" by former US President "Mr. Obama" [3]. Another similar oil spill incident occurred on 15 January 2022 in Peru, where approximately 6000 barrels of oil were spilt over 700 hectares of water, threatening aquatic plants and animals. Ultimately, oil spills in oceans and seas cause a potential risk to climate stability, environmental problems, and loss of ecology [4, 5]. Therefore, to tackle such a problem, different conventional methods like chemical coagulation, biological treatment, centrifugation, physical adsorption, and skimming were explored by researchers [6, 7]. These approaches are critical for reducing the environmental effects of oil spills and preserving the integrity of natural ecosystems. Despite their ubiquitous application, these technologies exhibit notable limitations, such as high operational costs, excessive energy requirements, low separation efficacy, and consequential environmental deterioration due to the release of toxic gas emissions into the atmosphere [8, 9].

Consequently, scientists have developed novel approaches that are economically viable and highly efficient to surmount these constraints for the effective separation of oil from water [10]. However, oil spillage remains a menace for researchers and is still considered one of the most significant factors of water pollution [11]. There has been growing interest in developing material with enhanced wettability for oil–water separation [12, 13]. Moreover, most of the techniques to separate oil from water were inspired by natural entities like lotus leaves [14, 15], butterfly wings [16, 17], peanut leaves [18], red rose petals [19, 20], water strider legs [21], and fish scales [22, 23]. These natural entities possess low surface energy, which resists wetting, encouraging researchers to develop superhydrophobicity in engineering materials [24, 25]. Superhydrophobic surfaces exhibit unique surface properties, characterized by a WCA greater than 150° and a sliding angle smaller than 10°. The superhydrophobicity of the surface is dependent on both surface roughness and chemistry. The surface with hierarchical micro–nano-structures minimizes the adhesion forces, allowing water droplets to slide off the surface, contributing to the superhydrophobic behaviour [26]. The chemical composition of the surface with low surface energy materials minimizes the interaction between the surface and water molecules, promoting water repellency. Combining appropriate surface roughness with hydrophobic chemistry can synergistically enhance the overall superhydrophobicity [27–31].

This review article highlights recent advancements in OWS using porous super-wetting materials, primarily emphasizing the 3D-printed polymeric materials. One of the primary novelties of this work is to emphasize the limited application of low-cost additively manufactured environmentally friendly mesh that can replace the currently available metallic mesh. Most research considers metallic meshes as a filter primarily used for oil–water separation. Still, these meshes are expensive, complex to fabricate, and have limited design flexibility. This paper gives insight into the versatility of polymer-based 3D-printed mesh compared to conventional metallic mesh, their transformative capabilities, and adaptability with emerging manufacturing technologies. The report begins with the significance of water and the necessity for technological advances in the separation process. Furthermore, two methods (superhydrophobicity-superoleophobicity or superoleophobicity-superhydrophilicity) are explored briefly. The discussion concludes with a concise overview of current challenges and prospects in the fields of OWS based on recent findings. This review paper provides vivid insight into various 3D-printed polymeric membranes for OWS. Currently, most reviews primarily focus on additive manufacturing (AM) techniques in mechanical, aerospace, medical, and tissue engineering domains. However, the application of 3D-printed membranes and their potential in diverse OWS scenarios have not been extensively explored. Considering the mentioned research gap, the current contributions of AM technologies, highlighting the most recent developments and potential applications of polymer-based AM technologies for OWS, are explored briefly.

In summary, previous work illustrates that traditional OWS methods often rely on simple geometries and materials with limited customization capabilities. In recent works utilizing 3D printing technology, the approach to OWS has been revolutionized through innovative design, advanced materials, and enhanced functionality. These integrated features enhanced efficacy, durability, and reliability in the separation process. The creative work on OWS leveraging 3D printing technology represents a paradigm shift from conventional methods towards highly customizable, highly efficient, and sustainable solutions with advanced functionalities and improved performance. 3D-printed products designed using eco-friendly and recyclable materials, aligning with sustainable goals. Moreover, these separation devices with enhanced efficacy and performance contribute to reduced resource consumption and environmental impact over their lifecycle.

2 Different methods of filtering oily water

This section overviews different methods for filtering oily water, such as gas flotation, gravity settling, chemical coagulation, adsorption, membrane filtration, electrochemical, and centrifugation [32–34]. The chemical processes frequently need highly skilled operators, substantial operating expenses, and continuous process monitoring control [35]. Oil pollution droplets can be floated in water using gas flotation techniques such as sparging or dissolved gas floatation. Gas flotation systems create agglomerates; gas bubbles adhere to dispersed oil droplets when injected. Researchers have made significant progress in utilizing surfactants as a promising approach to enhance the extraction of oil droplets from water. The gas floatation approach is superior for oil concentrations below 1000 mg/L [33]. Although centrifugation consumes a significant amount of energy, it successfully segregates oil from an oil–water mixture (OWM), mainly when the densities of the two liquids are similar [36]. Coagulation is a very adaptable technology utilized extensively for oily wastewater. This technique dissolves emulsified oils by combining colloids and suspended particles to form bigger flocs that may be removed from the system [37]. Even though the coagulation approaches are effective, the wastewater's composition impacts the coagulant's concentration, and this expensive approach leads to the generation of secondary pollutants that menace aquatic species. As a result, it is recommended to utilize electrocoagulation to enhance coagulation processes by generating separation force. The electric field accelerates coalescence and the movement of water particles towards the electrodes, whereas gravity forces are more efficient at removing bigger agglomerates. Adsorption is a cheaper, more efficient, and space-intensive approach for OWS. Conventional absorbers used in the OWS process, such as wool, zeolites, and activated carbon, may have various issues, including inadequate selectivity, low wettability, and recycling concerns [38]. The choice of method depends on factors such as the type and concentration of the oil, the volume of water, regulatory requirements, and economic considerations. So, it is crucial to conduct a thorough assessment of the specific conditions and requirements before selecting a filtration method for oily water treatment. Table 1 illustrates the summary of the different methods for filtering oily water. In the subsequent section, the investigation of wettability and understanding of surface phenomena is discussed briefly.

Table 1 Comparison between different methods of filtering oily water

Treatment	Advantages	Disadvantages	Driving forces
Gas Flotation	Potent filtration Environment friendly Easily accessible	Requires ample space Stagnant dissolution	Solvability
Gravity settling	Extracting heavy lubricants Eco-friendly Cost-effective	Ineffective for high-density liquids	Density discrepancy
Coagulation	Effective filtration The ability to combine flexibility and flotation for improved separation effectiveness	Costly operations Secondary pollution problem Reliant on a skilled operator	Density difference
Adsorption	Low-cost and low-energy consumption process Minimal chemicals consumption High oxygen demand for chemicals and oil removal	Low efficiency Low hydrophobicity High confinement time Secondary pollution problem	Vander Waal force
Membrane filtrations	Fast separation Pressure reliant	Fouling problem Expensive	Size
Electrochemical	The regulated thickness of the coating	Corrosion of the electrodes	Response to oxidation and reduction
Centrifugation	Efficient for free and dispersed oil	Intense energy consumption Prolonged process	Centrifugal force

3 Membrane wettability phenomena and their function

The wettability of a membrane is an essential aspect that impacts diverse phenomena and functionalities in membrane-based processes. Wettability refers to the ability of a liquid to spread and adhere to the surface of a solid material. It is a critical property influencing various phenomena and functionalities in different applications, particularly in materials science, chemistry, and engineering. The degree of wettability is determined by the balance between cohesive forces within the liquid and adhesive forces between the liquid and the solid surface. The wetting properties of the surface depend upon factors such as surface roughness, chemical composition, surface energy, and the nature of the liquid play crucial roles in determining the wettability of a surface [39, 40]. Understanding and controlling wettability is essential in designing materials and surfaces with specific characteristics, such as superhydrophobicity or enhanced adhesion. Surface treatments can alter the wetting behaviour of materials for particular applications in creating self-cleaning surfaces, water-repellent coatings, and adhesion-promoting treatments. The contact angle technique is utilized to evaluate the wettability of these surfaces [41, 42].

3.1 Contact angle method

The contact angle method is used to assess the wettability of a solid surface by a liquid. It measures the angle formed at the intersection of the liquid–air interface and the solid surface. The contact angle is crucial to explaining how well a liquid spread and adheres to a solid material. In wettability, a higher contact angle indicates a less wettable surface (hydrophobic or oleophobic), while a low contact angle suggests a more wettable surface (hydrophilic or oleophilic). This method is widely employed in various scientific and industrial fields, including materials science, surface engineering, and biomaterials research. It helps researchers and engineers understand the wetting properties of surfaces, contributing to the development of products with specific functionalities, such as self-cleaning surfaces, water-repellent coatings, and adhesion-promoting treatments. The sessile drop method is the most prominent for measuring contact angles in determining wettability [43, 44]. It entails measuring the angle between the liquid–solid interface and a tangent line drawn at the point of contact. According to Young's equation, the wetting regime may be separated into three groups based on the contact angle: water-wet, intermediate-wet, and oil-wet states. Conversely, a large contact angle indicates poor wetting, with the liquid-forming droplets exhibiting minimal surface coverage. Figure 1 shows that a surface is hydrophilic when the WCA is less than 90° and hydrophobic when it is more than 90° [45].

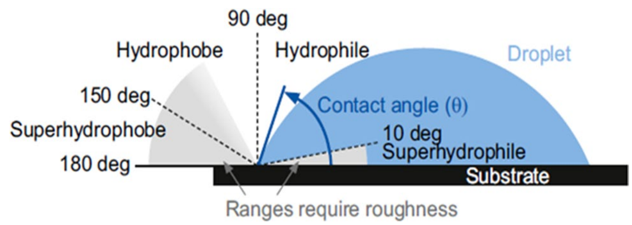

Fig. 1 The Contact angles of different wetting properties [45]

The sessile drop method is well known for its ease of use and efficacy, especially when evaluating flat surfaces [46, 47]. However, real-world surfaces are often rough, heterogeneous, and porous, which poses challenges in applying this method [47, 48]. The superhydrophobic surface exhibits advantageous properties owing to its uneven and rough topography. The surface features micro–nano-structures and nano-enclosed pores, introducing height variations that result in air bubbles' entrapment. The Wenzel model is a theoretical framework used to describe the wetting behaviour of a liquid on a rough or textured surface. The Wenzel model is applicable for homogenous surfaces, as shown in Eq. (1). Scientists have researched the chemical aspects of non-stick and anti-adhesion coatings, employing the Cassie–Wenzel hypothesis, as shown in Eq. (2) [49]. Understanding and controlling membrane wettability is critical for designing membranes with desired functionalities. By manipulating wettability, researchers and engineers can improve membrane performance in filtration, antifouling, and selectivity for various other applications. The mechanism and factors that affect the membrane design for OWS application are discussed briefly in a subsequent section.

$$\cos\theta_w = r\cos\theta \tag{1}$$

where θ_w = Wenzel angle of contact, θ = Young's angle of contact, and r = surface roughness factor. For heterogeneous surfaces, Cassie and Baxter's model is applicable by Eq. (2):

$$\cos\theta = f_1\cos\theta_1 + f_2\cos\theta_2 \tag{2}$$

where θ = angle of contact, f_1 = ratio of solid to liquid contact area, and f_2 = contact area ratio with air packets that confine the inner side of surface cavities.

4 Mechanism of OWS and design strategies of membrane

Superhydrophobic surfaces have unique surface properties that make them extremely adaptable to various applications such as self-cleaning, anti-fogging, antifouling, and material drag reduction [50, 51]. Numerous strategies have been employed to address the challenges associated with oil–water mixture (OWM). These methodologies aim to manage diverse repercussions by utilizing materials designed to selectively facilitate the passage of one wetting liquid while impeding the flow of another. The effectiveness of this separation is contingent upon the mechanism of oil and water blocking. Optimal selection of a separating medium is crucial for allowing the preferential passage of one wetting liquid while impeding the flow of another, typically achieved through gravity-driven processes. In OWM separation, hydrophobic or superhydrophobic surfaces are commonly utilized to prevent water permeation. These surfaces, characterized by low surface energy and distinctive micro- or nanostructures, repel water. Water passage is hindered by incorporating such features into porous materials, while oil can selectively flow through the pores.

On the contrary, a surface exhibiting hydrophilic or superhydrophilic properties is suitable for effectively repelling oil and maintaining separation from water. The choice of surface characteristics plays a crucial role in achieving efficient and selective separation of OWM. Size-sieving and demulsification are two essential processes involved in isolating emulsified OWM, are shown in Fig. (2). Size-sieving is based on the difference in molecule sizes between water and oil, and materials with superhydrophobic-superoleophobic (SHSO)

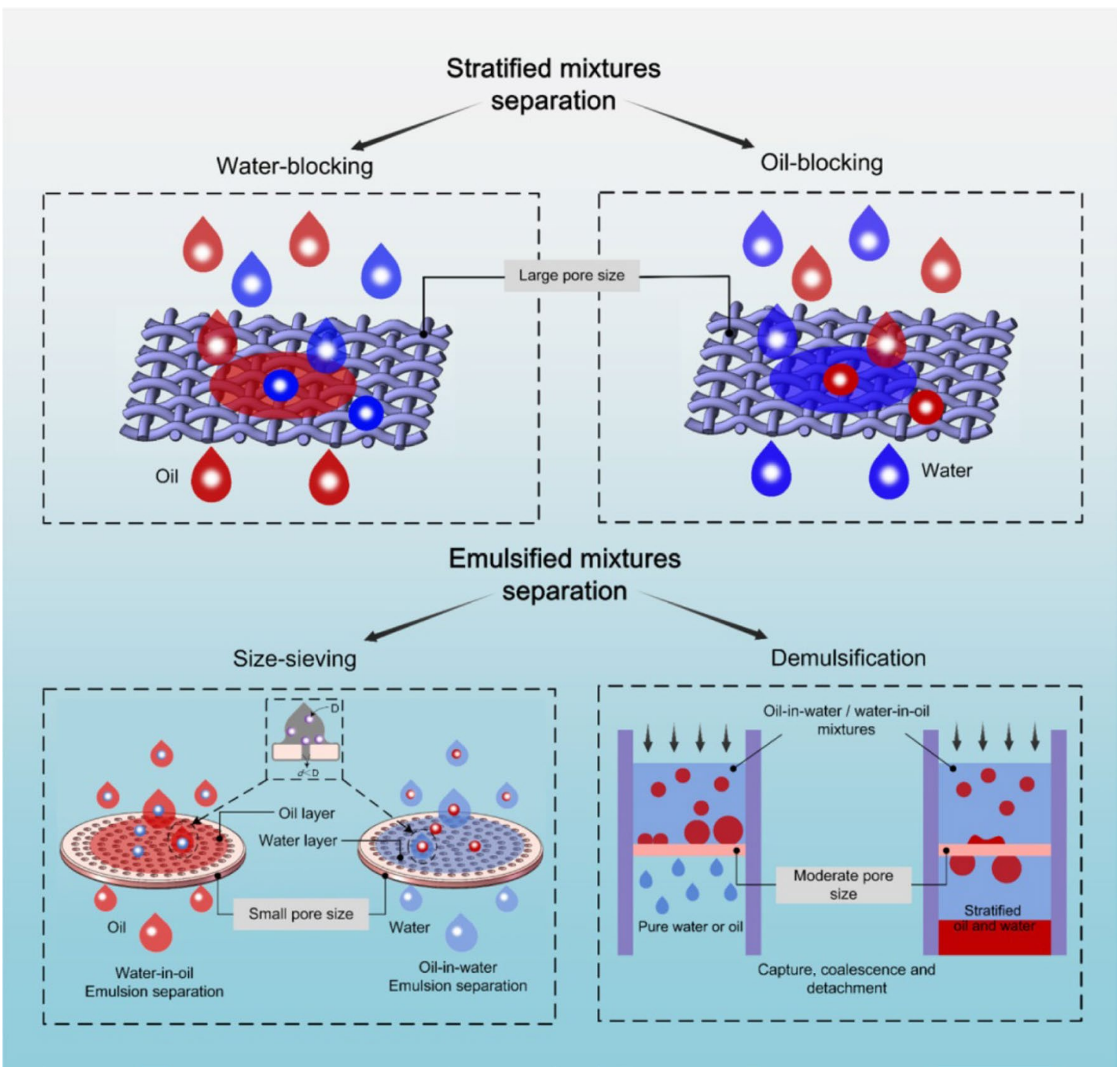

Fig. 2 Mechanism of oil–water separation [52]

properties have been used to separate oil from water. Conversely, demulsification is an intriguing separation approach in which certain chemicals help break the emulsion [52, 53]. The membrane's separation design depends on pore size and breakthrough pressure, allowing efficient separation depending on these characteristics.

4.1 Critical factor affecting membrane for OWS

In the systematic design of porous materials for OWS, two critical physical parameters affect surface structure: pore size (porosity) and breakthrough pressure. The surface structure, precisely the pores' size and distribution, influences the material's ability to selectively adsorb or repel certain substances, such as oil or water. Porosity determines the overall volume of the material available for fluid interaction and permeation. Additionally, the breakthrough pressure represents the point at which the applied pressure exceeds the material's capacity to retain the desired fluid, leading to potential leakage or compromised separation performance. By carefully considering and optimizing these physical parameters, researchers can enhance the design of porous materials for efficient OWS applications.

4.1.1 Pore size

The size of the membrane pores primarily determines the separation performance for OWS. The bubble pressure test is the standard technique for measuring membrane pore sizes. It works on the capillary action of liquid in the membrane pores. This test provides information about the most prominent pores in a membrane and helps characterize microfiltration and ultrafiltration membranes. It aids in quality control and ensures that membranes are suitable for specific OWS filtration applications. Other methods for determining membrane pore size include computer tomography, gas adsorption, porosimeter testing, and mean-flow pore size methods. Computer tomography is a medical imaging technique that uses X-ray tools for visualizing the internal structure and characteristics of the membranes including details about pore size, shapes, and distribution. This information is crucial for understanding and optimizing the performance of membranes in OWS applications. Another technique is gas adsorption used to characterize membranes' surface area, porosity, and pore size distribution. It involves exposing a material to a gas and measuring the amount of gas adsorbed as a function of relative pressure. It provides information for understanding the structural properties of membranes and is often used in research and quality control processes related to membranes. Porosimeter testing measures the pore volume and pore size distribution of porous membranes. It is based on the principle that the liquid volume is displaced to the membranes' pores. It provides information crucial for understanding the structural properties of membranes in the applications of OWS. Another method is mean-flow pore size techniques to determine the average pore size of the membranes. These above methods help understand the structural properties of membranes and are commonly used in research, development, and quality control in OWS. It assesses the flow of liquid through a membrane at varying pressures and results in information to calculate the average pore size of the membranes. Furthermore, it should be noted that the membrane's pores exhibit irregular shapes and sizes, including their pore size and surface area [54, 55]. Finally, understanding and controlling the mean pore size of a membrane is crucial aspects of membrane technology. It allows for optimizing separation processes by tailoring membranes to the specific requirements of the intended application, ensuring efficient and precise filtration based on their pore sizes. Understanding pore size is essential in establishing an environment that optimizes the precision of particle size information throughout the separation procedure.

4.1.2 Breakthrough pressure

The critical pressure (Pc), also referred to as the breakthrough pressure (P_b), holds significant importance as a fundamental physical property in membrane design. It is commonly known as the liquid entry pressure (LEP) and is considered the maximum pressure that must be applied to a membrane before liquid seeps into the pores. The determination of breakthrough pressure often involves observing the initial droplet formation on the membrane, and the widely used Young–Laplace method is employed to measure this phenomenon [56, 57]. Researchers, including Franken et al., Kim, and Harriott-Zha, have developed models with the same objective. These models aim to determine the breakthrough pressure (Pc) of cylindrical structures possessing small, uniformly sized pores. The breakthrough pressure obtained by Eq. 3 is shown below:

$$\Delta P_{\mathrm{c}} = \frac{-2\gamma_L \cos\theta_L}{r_{\mathrm{P}}} \tag{3}$$

where γ_L = surface tension of the fluid and r_{p} = maximum pore radius of the membrane.

As mentioned earlier, Young's equation is limited to ideal surfaces and cannot be extended to actual surfaces, such as the rough surface of a membrane. In contrast, the Laplace–Young equation accounts for the influence of membrane wettability, which can significantly affect the pressure-driven membrane filtration process. Consequently, the expression governing surface wettability and breakthrough pressure may require modification. The fabrication of membranes using various techniques has been considered to separate oil from water effectively. These processes involve developing membrane materials with tailored properties and structures to enhance their OWS capabilities.

5 Fabrication of metallic membrane filter and its application

In recent years, substantial scientific steps have been undertaken to explore the potential applications of metallic meshes in the field of OWS. The advantages of metallic mesh are their ease of access, cost-effectiveness, and porous mesh structure, enabling a high flux rate and ensuring optimal separation efficacy. Various metallic meshes, such as stainless steel, copper, and others, have been used for separation due to the surface characteristics and affinity of materials. The surface properties of mesh material can be enhanced by hydrophobic or hydrophilic polymeric coating on their surface. The applications of polymeric coating on metallic mesh substrate for OWS are explored briefly in a further section.

5.1 Fabrication of polymeric coating on a metallic substrate for OWS

Scientists have successfully constructed metallic membranes for OWS by using changes in interfacial energy between oil and water [58]. These membranes are made of mesh and have hydrophobic or hydrophilic properties, allowing them to operate as "oil-removing" or "water-removing" materials. However, it should be noted that these meshes are only suited for use in mild environments since they are prone to corrosion and are vulnerable to harm from acidic, alkaline, or salt solutions [59]. In the subsequent section, polymer coating on stainless-steel and copper mesh material is discussed briefly for OWS applications. Researchers have been interested in using metallic mesh for OWS since the publication of Feng et al. [60] in 2004. In their study, the authors established a uniform dispersion of polytetrafluoroethylene (PTFE) particles (30 wt. %), polyvinyl acetate (PVAC) as an adhesive (10 wt. %), sodium dodecyl benzene sulphonate (SDBS) as a surfactant (2 wt. %), and thinner sprays (50 wt. %) to coat stainless-steel (SS) mesh. The stainless-steel mesh was cleaned before applying the coating solution by spraying and curing the sample at 350 °C. The coated mesh has a WCA of 156.2° and a sliding angle 4°. This proposed technique, however, has received criticism because of its poor thermal and mechanical stability. Nonetheless, it has been observed that PTFE-coated SS meshes exhibit superhydrophobicity characteristics, resulting in good OWS performance. PTFE inherently possesses hydrophobic properties, with a WCA ranging from 98° to 112°. Notably, PTFE's exceptional chemical resistance can make dissolving in a solvent for electrospinning applications challenging [61].

Since then, several researchers have worked together to create wettable membranes that may be used for OWS. Qin et al. [62] altered Feng's experimental method by utilizing PTFE suspension, adding polypropylene sulphide (PPS), and obtaining a similar WCA of 156°. Several researchers used immersion techniques to provide the metallic mesh with SHSO characteristics by altering their surfaces with stearic acid (CH_3 $(CH_2)_{16}COOH$). Researchers employed stearic acid to construct SHSO features on SS mesh in various works using nanoparticles such as Mg $(OH)_2$, Cu crystals, and ZnO. In another study, Khosravi et al. [63] created a superhydrophobic surface on SS mesh by deposing polypyrrole and carbon soot nanospheres on the mesh surface, followed by surface modification with stearic acid and obtained a separation efficacy of 99% after 50 cycles. Guo et al.[64] reported that epoxy/hexadecyltrimethoxysilane halloysite nanotubes (HDTMS-HNTs) were sprayed onto SS mesh to create a superhydrophobic halloysite-based mesh that can successfully separate a variety of OWM with a separation efficacy of over 98.6%. The HNTs treated with Hexadecyltrimethoxysilane (HDTMS) enhance the mesh's surface roughness and superhydrophobic characteristics. The mesh maintains a static WCA of 154° and sliding angles of 1.5° even after 25 separation cycles. In another study, Guo et al. [65] applied a polyhedral oligomeric silsesquioxane (POSS) hybrid acrylic polymer coating on SS mesh for OWS applications. The coated mesh exhibits a WCA of 153° and a sliding angle of 4.5° after undergoing 25 separation cycles with a separation efficacy of 99%. In other works, Zhang et al. [66] developed an SHSO surface on SS mesh by immersion technique to grow a hierarchical ZnO micro–nano-structure for OWS. The coated mesh revealed a WCA of 156° and a separation efficacy of 95% after ten separation cycles. These functionalized membranes perform admirably in harsh operational scenarios such as corrosive environments, acidic and basic environments, and saline solutions. Zhang et al. [67] developed an efficient and robust superhydrophilic coating for OWS on SS mesh. Figure 3 shows SEM images of both coated and uncoated mesh, along with XRD and EDS analysis. In Fig. 3 a–b, the uncoated mesh displays interwoven pure steel wires to form a regular reticulated surface. In contrast, the coated mesh shown in Fig. 3 c–e exhibits an abundance of microstructure particles characterized by irregular cube-like structures that facilitate the creation of a unique wettability surface. On the surface of the mesh, as shown in Fig. 3 f–i, an EDS revealed the presence of only Mn, Co, and O elements that conform coating of $MnCo_2O_4$ on SS mesh. The $MnCO_2O_4$-SSM (Manganese Cobalt Oxide-Stainless-Steel Mesh) achieves exceptional antifouling properties with a WCA of 156°, separation efficacy of 99.9%, and high flux rate of 63 Lm^{-2} h^{-1}. The $MnCO_2O_4$-SSM exhibits superior recycling stability, maintaining its performance after 30 separation cycles.

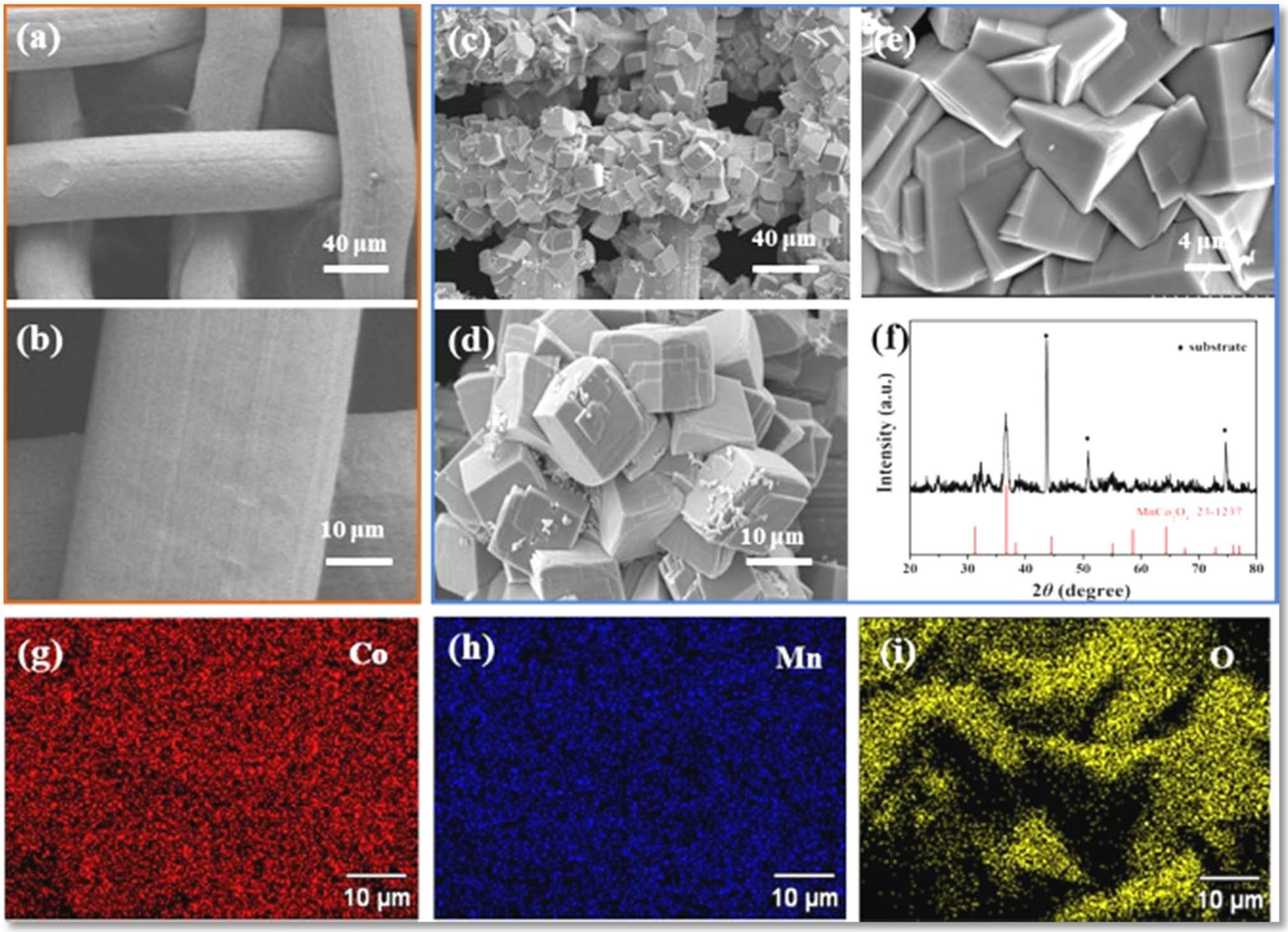

Fig. 3 SEM images of SS mesh at various magnifications: both **a**–**b** pure SSM, **c**–**e** SSM coated with $MnCo_2O_4$, **f** XRD patterns of $MnCo_2O_4$-SSM, and **g**–**i** EDS mapping of the $MnCo_2O_4$-SSM [67]

Table 2 Summary of stainless-steel mesh substrate for OWS

Deposited materials	Methods	WCA	Efficiency (%)	Separation cycle	References
Polytetrafluoroethylene	Spray	156.2 ± 2.8°	–	–	[60]
Carbon soot	Combustion flame	–	99	50	[63]
HDTMS-HNTs	Spray	154°	98.6	25	[64]
POSS	Spray	153°	99	25	[65]
ZnO	Immersion	156°	95	10	[66]
$MnCO_2O_4$	Dip	156°	99.9	30	[67]

Using stainless-steel mesh (SSM) as an OWS substrate has significant implications for treating and reusing petrochemical effluents. Table 2. highlights the stainless-steel mesh substrates employed in OWS, indicating their excellent separation efficacy and recycling stability, ensuring long-term performance through several cycles. Extensive research has also been undertaken on using superhydrophobic coatings on metallic mesh for OWS, particularly copper mesh. These coatings attempt to improve metallic meshes' separation efficacy and performance by generating a superhydrophobic surface. The extensive exploration of superhydrophobic coatings on metallic mesh, particularly copper mesh, advances OWS technologies and broadens the materials suitable for such applications. [68, 69]

Cao et al. [70] created micro–nano-hierarchical structures on the copper mesh using electrodeposition and immersion procedures. The coated mesh exhibits a WCA of 152.4°, a sliding angle of 12.6°, and a high oil flux rate

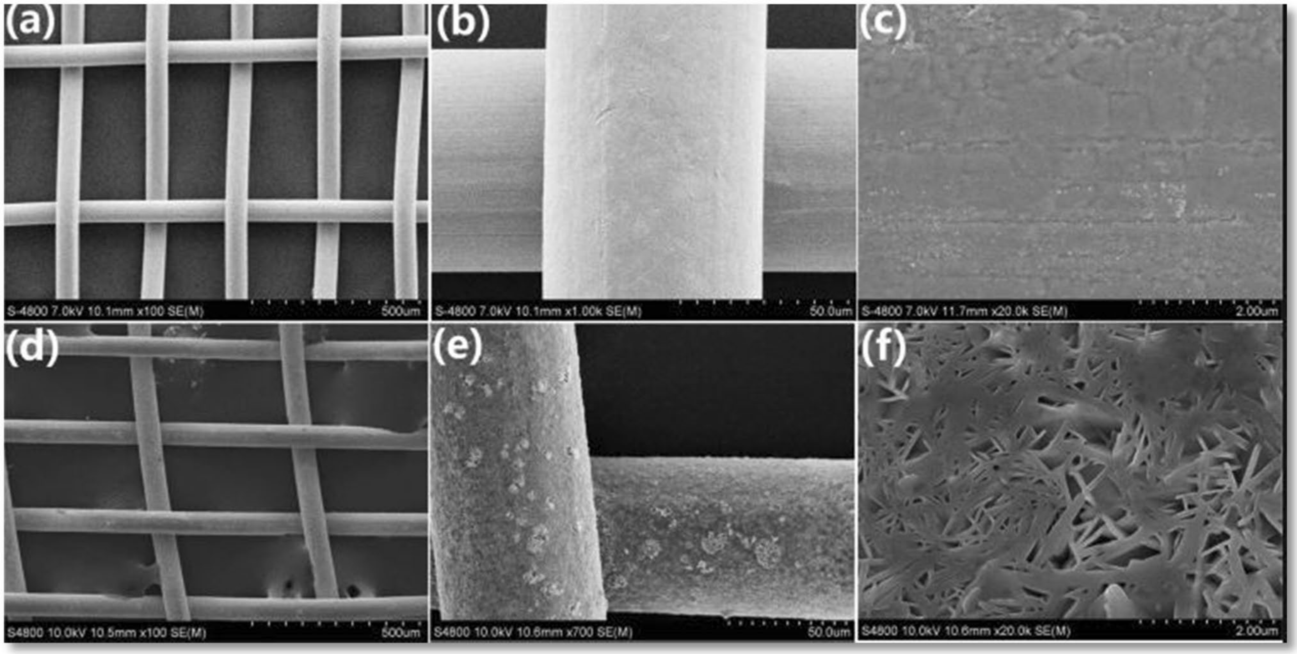

Fig. 4 **a–c** SEM images of bare copper mesh and **d–f** coated copper mesh [70]

of 4507 Lm^{-2} h^{-1} with 90% separation efficacy. Figure 4 shows SEM images of copper mesh surfaces before and after coating. Figure 4 a–c shows that the bare copper mesh surfaces exhibit relatively smooth characteristics. Conversely, Fig. 4 d–e reveals the presence of rough micro–nano-wire structures on the coated surface, indicating the successful implementation of the electrodeposition method. The coating on the mesh surface shows a remarkable increase in hydrophobicity.

In other works, Liu et al. [71] coated the copper mesh for OWS applications using the electrodeposition process. The coating on the mesh surface shows a WCA of 155.5° with a separation performance of 93% for various OWM. These remarkable surface properties, including high WCA and complete oil wetting, were retained after ten separation cycles. In another study, Zhang et al. [72] employed the CVD technique to coat copper mesh with silica particles for OWS applications. After being modified with hexamethyldisilane (HMDS), the PSCCM-coated membrane shows SHSO properties. The coated mesh exhibits 98% separation efficacy even after 300 separation cycles with a gravity-driven system.

Similarly, Khosravi et al. [73] earlier used SS mesh and, in a further study, used copper mesh for OWS. In his research work, authors have used a hydrothermal approach for the first time to develop a superhydrophobic CuxS/Cu ($x = 1, 2$) mesh, followed by modification with stearic acid for OWS. The coated mesh exhibits a WCA of $160° \pm 1°$ with a separation efficacy of 99.9% even after 100 cycles. The developed superhydrophobic CuxS/Cu mesh has significant potential for in situ OWS and is easily accessible for collecting organic contaminants and spilt oil. In recent work, Luo et al. [74] produced extremely hydrophilic nickel nanoparticles with a core–shell shape for coating the copper mesh by electrodeposition method. The developed mesh exhibits an OCA of 155°, with a separation efficacy of 98% after seven cycles.

In a further study, You et al. [75] reported coating on copper mesh with deposition of Zn–ZnO to develop a highly hydrophilic structure. The electrodeposited copper mesh featured a flower-like hierarchical structure with underwater OCA of 155.6° and separation efficacy of 99%. The durability and anti-corrosive properties of the copper mesh make it suitable for treating complex industrial oily wastewater. The separation device based on this copper mesh holds promising potential for addressing challenging environmental pollution issues related to oil contamination. Lastly, the primary approach employed in the utilization of copper mesh for OWS involves the creation of rough surfaces, leading to exceptional wettability.

These modified meshes exhibit surface patterns reminiscent of natural structures observed on water skippers and lotus leaves. Graphene oxide, carbon nanotubes, and dopamine enhance the copper mesh's mechanical and photocatalytic performance [76, 77]. Table 3 illustrates the summary of the copper mesh substrate for OWS. Researchers have further turned to polymeric mesh fabricated using additive manufacturing techniques to overcome the corrosion

Table 3 Summary of copper mesh substrate for OWS

Deposited materials	Methods	WCA	Efficiency (%)	Separation cycle	References
n-dodecyl mercaptan and tris(hydroxymethyl) Amino methane hydrochloride	Electrodeposition	152.4°	> 90	–	[70]
Sulphuric acid-copper sulphate	Electrodeposition	155.5°	93	10	[71]
Silica	Chemical vapour deposition	158°	98	300	[72]
Cu_xS-Stearic acid	Hydrothermal	160°	100	100	[73]
Nickel nanoparticles	Electrodeposition	155°	98	7	[74]
Zn/ZnO	Electrodeposition	155.6°	99	50	[75]

associated with metallic mesh filters used for OWS. These polymeric meshes offer excellent corrosion resistance and can efficiently separate oil and water phases. Polymeric meshes with higher durability, chemical resistance, and superior separation efficacy may be created through additive manufacturing, making them well suited for OWS applications.

6 Application of additively manufactured membrane

Additive manufacturing, also known as "3D printing", produces 3D objects by depositing materials in a layer-by-layer mode with the help of CAD design. It helps fabricate customizable products and intricate structures in a single step with nil material wastage. Moreover, it has the benefits of accessibility, flexibility, speed, sustainability, and risk reduction. It is one of the fastest-growing techniques and proves an alternative to traditional subtractive manufacturing due to its outstanding efficacy in terms of precision, performance, cost, and time [78, 79]. Hideo Kodama first developed the concept of 3D printing in 1981, where a photopolymer-based rapid prototyping method was used to build a 3D model using ultraviolet (UV) light. Since then, several innovative additive manufacturing methods have been developed rapidly, which include stereolithography (SLA), fused deposition modelling (FDM), and selective laser sintering (SLS). It has been noticed that this technology has increased in the past few decades, and most of the work has been published in tissue engineering, biomedical, aerospace, etc. A variety of thermoplastic polymers like acrylonitrile butadiene styrene (ABS), polystyrene (PS), polycarbonate (PC), nylon, high-density polyethylene (HDPE), polylactic acid (PLA), etc., were used in 3D printing processes like FDM and SLS for part fabrication. Still, 3D printing in membrane

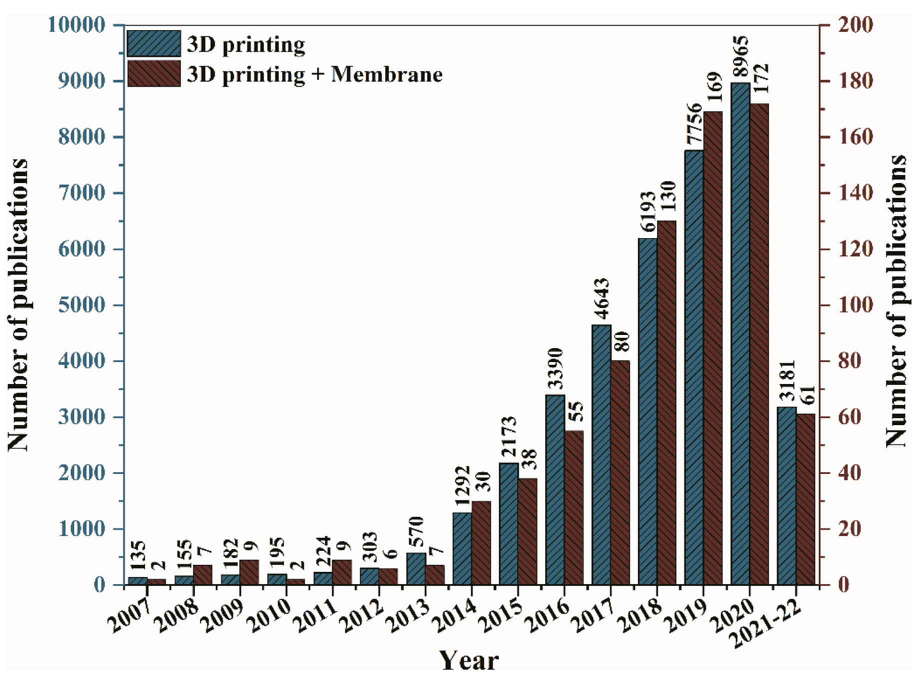

Fig. 5 Publication trends from 2007–2022 in 3D printing and 3D printing membrane [80]

separation is a new and challenging research field for OWS. Figure 5 shows an exponential rise in the number of publications related to 3D printing from 2007 to 2022. Still, there have been few publications in recent years on OWS using additive manufacturing. Therefore, scientific communities have shown keen interest in developing membranes using additive manufacturing for OWS in recent years.

6.1 Fabrication of polymeric coating on the 3D-printed membrane for OWS

The quantity of water increases as the world population grows, but water quality is declining steadily. As explained earlier, the primary source of water pollution is frequent oil spill accidents during excavation, extraction, and transportation, posing significant environmental challenges. The primary concern is effectively separating oil from the water after such incidents. Earlier, various conventional methods were used to clean water, but they were not much efficient. Contrary to traditional manufacturing techniques, 3DP has been employed to develop nearly perfect porous membrane structures with the required OWS characteristics. This approach empowers the creation of intricate shapes and customizable structures, enabling the design and production of efficient separation devices tailored to specific applications. The utilization of additive manufacturing techniques in OWS has demonstrated the potential to achieve enhanced separation efficacy, improved selectivity, and reduced costs compared to traditional manufacturing methods. By changing the design flexibility offered by additive manufacturing, it becomes possible to fabricate complex porous structures, customize surface properties, and optimize flow paths within separation devices.

Additionally, additive manufacturing allows for incorporating functional features such as hydrophobic or hydrophilic coatings, precise control over pore sizes, and size-sieving capabilities within the separation devices. These features can enhance the performance and adaptability of the separation process, facilitating the effective removal of oil from contaminated water. Researchers have proposed various materials, including polymers and ceramics, to coat substrate surfaces with micro–nano-scale superhydrophobic structures, thereby enhancing the OWS properties [81]. Lv et al. [82] have used 3D-printed superhydrophobic structures at microscopic and nano levels for OWS. The mesh structure was 3D printed with polydimethylsiloxane (PDMS) ink containing hydrophobic nano-silica for the OWS. The incorporation of nano-silica in PDMS solution improves the printability as well as the mechanical characteristics of the sample. The 3D-printed membrane of pore size 0.37 mm has a high oil flux of 23,700 LMH. The printed membrane has a WCA of 158° with a separation efficacy of 99.6%. The 3D printing method incorporates the superhydrophobic surface into the porous framework, thus eliminating the weaker interfacial adhesion problem that occurred with conventionally prepared superhydrophobic membranes. The superhydrophobicity of the membrane was created by "coating on a mesh structure", adjusting the ink rheology, and generating the desired porous structure. In another study, a 3D-printed porous structure was prepared using PLA filament via the FDM technique. The samples were coated using methyl-ethyl-ketone (MEK) solution etching with hydrophobic nano-silica (HN-SiO_2) and low surface energy fluorosilane modification at different wettability for OWS. The cylindrical sample was designed by UG NX 12.0 software, having three kinds of holes containing side lengths of 0.8, 1.0, and 1.2 mm for OWS fabricated, as shown in Fig. 6. The outcomes demonstrate OWS with a side length of 1.0 mm has better separation efficacy with a high flux rate [83].

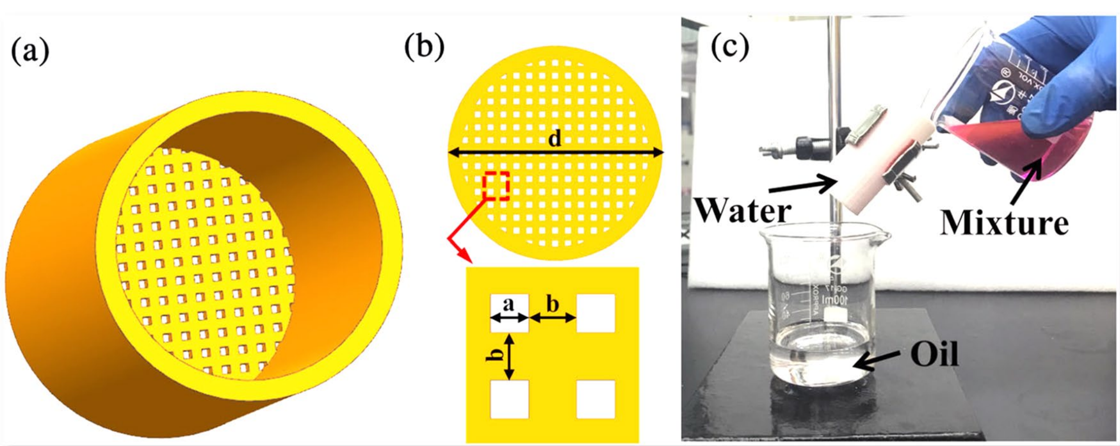

Fig. 6 **a** 3D model of a cylindrical OWS designed by UG NX12.0 software and **b** Porous bottom surface **c** OWS using 3D-printed cylindrical membrane [83]

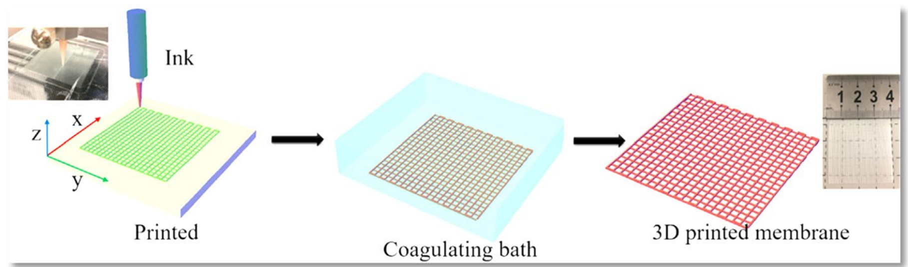

Fig. 7 Preparation of 3D-printed composite membrane [85]

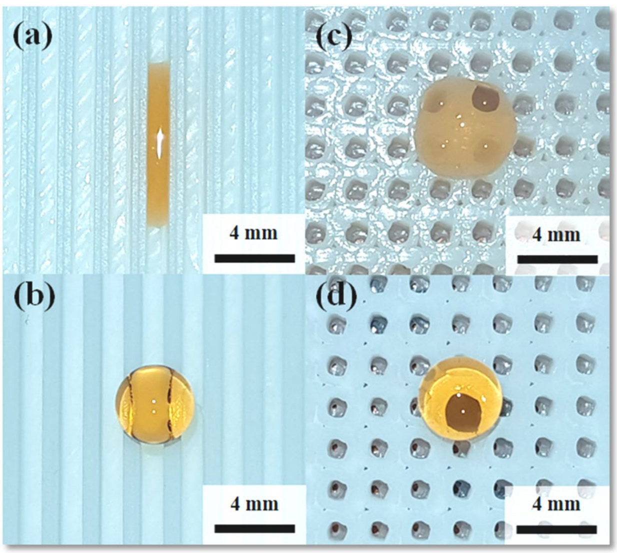

Fig. 8 Optical microscopic image of the water droplet on a surface having 1.0 mm of step size **a–b** uncoated samples and **c–d** dip-coated samples [86]

Similarly, Xin et al. [84] fabricated a 3D porous film via the FDM technique and immersed it in acetone to develop a flower-like surface. Furthermore, the structure was dipped in dopamine buffer containing polystyrene nanospheres to create superhydrophobic behaviour. It was observed that after dip coating surface exhibits a WCA of 151.7°, low water adhesion force of 21.8 μN, maximum efficacy of 99.4% with a pore size of 250 μm, and a high flux of 60 kLm^{-2} h^{-1}. Li et al. [85] have used the direct inkjet writing (DIW) technique to create a superhydrophilic and underwater superoleophobic membrane with an ordered porous structure for OWS. The ink fabricating the membrane was a solid-like solution made of cellulose acetate (CA), poly-(vinyl alcohol), and silica nanoparticles. The fabrications of 3D-printed porous membranes are shown in Fig. 7. It was observed that after 50 cycles, a separation efficacy that was driven by gravity was found to be approximately 99.0%, with WCA in the air of about 18.14 ± 2.61° and OCA underwater of about 159.14 ± 0.59°, thus showing superhydrophilic and superoleophobic characteristics for OWS.

In another study, Lee et al. [86] used FDM 3D printing with PLA filament to fabricate a mesh structure. They coated it with silica nanoparticles through a dip coating technique to create a superhydrophobic surface. The line and grid pattern were 3D printed, as shown in Fig. 8. As shown in Fig. 8, a and c show uncoated bare samples, and it can be noticed that water droplets wet the surface. As shown in Fig. 8 b and d, dip-coated samples were water droplets rolled on the surface, showing superhydrophobic characteristics that can be used for OWS applications.

Yang et al. [87] fabricated eggbeater heads with superhydrophobic micro-scale artificial hairs inspired by salvinia molesta leaf. The structure was aided with the 3DP technique for adjustable hydrophobicity and mechanical endurance of the microstructure, which has exhibited 99.9% OWS. Similarly, in another study, 3D-printed polysulfone (PSU) membranes were covered with candle soot, and it was observed that the structure exhibited separation efficacy greater than 99% for a mixture of hexane/water [88]. Xing et al. [89] reported the fabrication of 3D-printed superhydrophobic PLA packing for OWS. The superhydrophobicity of the sample was achieved through solvent etching and nanoparticle decoration. The 3D-printed PLA model was designed as a hollow cylinder, as shown in Fig. 9. It was noted that after acetone etching, the packing surface turned opaque, indicating a rough structure.

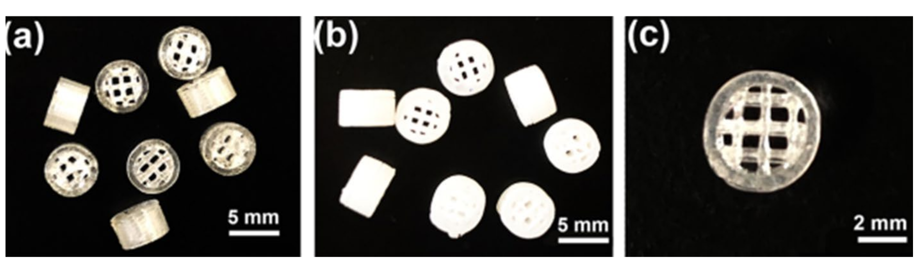

Fig. 9 Optical image of **a** and **c** additively manufactured PLA packing and **b** superhydrophobic PLA packing [89]

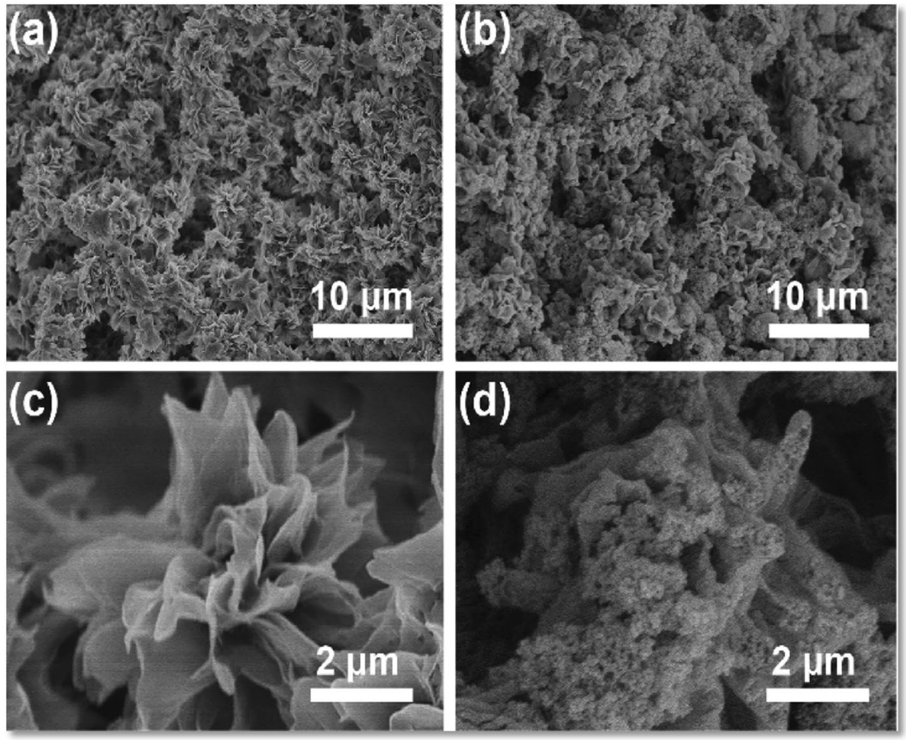

Fig. 10 Surface of PLA packing. by scanning electron microscopy **a–b** etched PLA packing and PS NP decorated PLA packing, respectively, and **c–d** respective magnified images [89]

The surface morphology of the packing is shown in Fig. 10. Figure 10 a and c illustrates a highly uneven surface with a denser micro-scale spherical rose petal structure after etching. Figure 10 b and d shows that micro/nano-hierarchical surface structures were observed after nanoparticle decorations. It was noted that PLA packing after the coating has a WCA of 150° and a water adhesion force of 22 μN. The maximum separation efficacy of 95% was obtained by exhibiting a high flux rate of 75 $kLm^{-2} h^{-1}$. Table 4 illustrates the summary of additively manufactured membranes for OWS.

7 Conclusion

The fundamental theories, recent advancements in materials, and design strategies for stratified and emulsified OWM are summarized. In each segment, a particular focus is dedicated to comparing separation efficiency and membrane flux rates in real-world industrial applications of oil–water separation. The advantages of additive manufacturing for the mesh design are summarized and compared with other metallic mesh for the OWS field. In comparison to other techniques like nano-imprinting, the application of a 3D-printed coating does not affect the size of the membrane surface nor decrease the number of pores on the surface. Moreover, 3D printing offers advantages such as speed, simplicity, cost-effectiveness, and excellent performance with micro-scale materials used in treating oily water. Although 3D printing has already appeared in many industries, integrating 3D printing with other fabrication processes is anticipated to enhance OWS's efficacy, transform it into an environmentally friendly product, and reduce its overall cost. This review also draws the following conclusions:

1) Superhydrophobic surfaces require nano- or micro-scale structures with low surface energy. In recent reports, 3D printing has been utilized to fabricate both micro-scale structures on the surface and nano-scale structures with low surface energy.
2) Among the most utilized surface modifications, silanes and chemical compounds like (thiols, stearic, lauric, and oleic acids) with extended functional groups are widely employed for surface modifications to enhance the performance of SHSO surface. However, the fluorine atoms in the functional groups may cause ecological problems.
3) The application of external forces and exposure to harsh conditions, including hot water, acidic solutions, brine, and alkaline solutions, can cause damage to the micro–nano-surface structures responsible for membrane superhydrophobicity. Consequently, guidelines are urgently needed to assess the long-term stability and durability of (SHSO) membranes under severe operating conditions.
4) The 3D-printed membrane exhibited notable mechanical stability, reusability, and high efficacy, making it suitable for a wide range of OWS applications.

The review findings indicate the potential customization of coatings on additive-manufactured membranes to

Table 4 Summary of additively manufactured membrane for OWS

S. no	Materials	Techniques/separation method	Pore size (mm)	WCA (degree)	Flux rate (KLMH)	Ƞ (%)	References
1	Superhydrophobic membranes using nano-silica filled Polydimethylsiloxane (PDMS) ink	Inkjet printing Membrane separation	0.37	158	23.7	99.6	[82]
2	PLA porous material, Methyl ethyl ketone (MEK) solution etching with hydrophobic nano-silica (HN-SiO_2)	Fused deposition modelling	0.8, 1, 1.2	–	–	–	[83]
3	Superhydrophobic porous film dip into dopamine buffer containing polystyrene nanospheres	Fused deposition modelling Gravity driven separation	0.25	151.7	60	99.4	[84]
4	superhydrophilic and underwater superoleophobic porous membrane cellulose acetate (CA), poly (vinyl alcohol), and silica nanoparticles	Direct ink writing (DIW) Membrane separation	–	159.14	–	99	[85]
5	Polylactic acid (PLA) filament and dip coating of the designed structure with silica nanoparticles	Fused deposition modelling	–	–	–	–	[86]
6	Egg beater heads with superhydrophobic micro-scale artificial hairs inspired by Salvinia molesta leaf	Submerged surface Accumulation based 3D (ISA-3D) printing Capillary force-based separation	–	–	–	99.9	[87]
7	Candle shoot functionalized polyamide-12 membrane	Selective laser sintering Absorption	–	–	–	99	[88]
8	Bio-inspired hollow Polydimethylsiloxane (PDMS) sponge	Inkjet printing Absorption	0.4	100–143	–	–	[90]
9	Superhydrophobic PLA packings polystyrene nanospheres	Fused deposition modelling Gravity driven separation	–	150	75	95	[89]

improve separation efficacy and various mechanical properties. Additionally, a diverse selection of biodegradable materials suitable for 3D printing is available, exhibiting specific improvements in properties. Furthermore, applying polymeric composite coatings on printed membranes has exhibited superior efficacy in separation processes. This review provides valuable insights for researchers in this field. It guides additive manufacturing industries, enabling them to understand the benefits of coatings on 3D-printed membranes and integrate the aforementioned findings into their work.

8 Future perspective

Possible improvements in wettability through modifications in the membrane for OWS open various opportunities for multiple applications, such as denser fluid separation and separation of fat cells in the blood. Further, there are still a few challenges in scientific and industrial communities, pointing to future research as follows:

1) The temperature, acidity, and alkalinity of actual oily effluent vary with each oil field and refinery. As a result, the resistance and stability of specific wetting materials should also be considered. The materials with cognitive responses are more suited for OWS in adverse environments.
2) River effluents or oily waste river water usually contain viscous oil and sand. The oil with high viscosity adheres to the surface of the 3D-printed mesh, and it is difficult to remove and thus reduces the efficacy after repeated use. Moreover, oily sand particles block the mesh, reducing separation efficacy.
3) The design and control of pore size from nanometres to microns are not accurate enough. Hence, further investigation on surface structure and OWS wettability must be studied.
4) The single super-wettability of separating material has certain limits in the application for separating stratified and emulsified OWM, whereas switchable wettability displays outstanding separation feasibility. Further, newer advancements in methods, theories, and the devel-

opment of unique wettability separating materials are currently undergoing a lot of research.

In short, a 3D-printed material allows low-cost fabrication that integrates separation and purification functions and can be recycled. Despite numerous barriers and drawbacks, the efforts in this field will enable enormous development and innovation in 3D-printed materials for OWS.

Funding The authors do not receive any financial support from any organization to carry out the present review.

Declarations

Conflict of interests The authors declare no potential conflicts of financial interest for this study's investigation, authorship, and publication.

References

1. Ge J, Zhao HY, Zhu HW et al (2016) Advanced sorbents for oil-spill cleanup: recent advances and future perspectives. Adv Mater 28:10459–10490. https://doi.org/10.1002/adma.201601812
2. Peterson CH, Rice SD, Short JW et al (2003) Long-term ecosystem response to the exxon valdez oil spill. Science 302(5653):2082–2086. https://doi.org/10.1126/science.1084282
3. Tuttle PL, Hemming JM (2019) Avian injury assessment for the Deepwater Horizon oil spill. Environ Monit Assess 191:1–4. https://doi.org/10.1007/s10661-020-08275-5
4. Qu M, Pang Y, Li J et al (2021) Efficient separation of oil-in-water emulsion based on a superhydrophilic and underwater superoleophobic polyvinylidene fluoride membrane. Surf Interface Anal 53:910–918. https://doi.org/10.1002/sia.6993
5. Shayesteh H, Norouzbeigi R, Rahbar-Kelishami A (2022) Evaluation of superhydrophobicity of chemical-resistant magnetic spiky nickel nanowires grafted with silane coupling agent for highly efficient oil/water separation. Surfaces and Interfaces 28:101685. https://doi.org/10.1016/j.surfin.2021.101685
6. Kang W, Guo L, Fan H et al (2012) Flocculation, coalescence and migration of dispersed phase droplets and oil-water separation in heavy oil emulsion. J Pet Sci Eng 81:177–181. https://doi.org/10.1016/j.petrol.2011.12.011
7. Kwon WT, Park K, Han SD et al (2010) Investigation of water separation from water-in-oil emulsion using electric field. J Ind Eng Chem 16:684–687. https://doi.org/10.1016/j.jiec.2010.07.018
8. Kabiri B, Norouzbeigi R, Velayi E (2022) Efficient oil/water separation using grass-like nano-cobalt oxide bioinspired dual-structured coated mesh filters. Surfaces and Interfaces 30:101825. https://doi.org/10.1016/j.surfin.2022.101825
9. Zhou W, Li G, Wang L et al (2017) A facile method for the fabrication of a superhydrophobic polydopamine-coated copper foam for oil/water separation. Appl Surf Sci 413:140–148. https://doi.org/10.1016/j.apsusc.2017.04.004
10. Chu Z, Feng Y, Seeger S (2015) Oil/water separation with selective superantiwetting/superwetting surface materials. Angew Chemie - Int Ed 54:2328–2338. https://doi.org/10.1002/anie.201405785
11. Qiu L, Sun Y, Guo Z (2020) Designing novel superwetting surfaces for high-efficiency oil-water separation: design principles, opportunities, trends and challenges. J Mater Chem A 8:16831–16853. https://doi.org/10.1039/d0ta02997a
12. Wan Z, Li D, Jiao Y et al (2017) Bifunctional MoS_2 coated melamine-formaldehyde sponges for efficient oil–water separation and water-soluble dye removal. Appl Mater Today 9:551–559. https://doi.org/10.1016/j.apmt.2017.09.013
13. Xue Z, Wang S, Lin L et al (2011) A novel superhydrophilic and underwater superoleophobic hydrogel-coated mesh for oil/water separation. Adv Mater 23:4270–4273. https://doi.org/10.1002/adma.201102616
14. Samaha MA, Tafreshi HV, Gad-el-hak M (2012) Comptes rendus mecanique superhydrophobic surfaces : from the lotus leaf to the submarine. Comptes Rendus Mec 340:18–34. https://doi.org/10.1016/j.crme.2011.11.002
15. Neinhuis C, Barthlott W (1997) Characterization and distribution of water-repellent self-cleaning plant surfaces. Ann bot 79(6):667–77
16. Niu S, Li B, Mu Z et al (2015) Excellent structure-based multifunction of morpho butterfly wings: a review. J Bionic Eng 12:170–189. https://doi.org/10.1016/S1672-6529(14)60111-6
17. Zheng Y, Gao X, Jiang L (2007) Directional adhesion of superhydrophobic butterfly wings. Soft Matter 3:178–182. https://doi.org/10.1039/b612667g
18. Darmanin T, Guittard F (2015) Superhydrophobic and superoleophobic properties in nature. Mater Today 18:273–285
19. Feng L, Zhang Y, Xi J et al (2008) Petal effect: a superhydrophobic state with high adhesive force. Langmuir 24:4114–4119. https://doi.org/10.1021/la703821h
20. Long J, Fan P, Gong D et al (2015) Superhydrophobic surfaces fabricated by femtosecond laser with tunable water adhesion: from lotus leaf to rose petal. ACS Appl Mater Interfaces 7:9858–9865. https://doi.org/10.1021/acsami.5b01870
21. Su Y, Ji B, Huang Y, Hwang KC (2010) Nature's design of hierarchical superhydrophobic surfaces of a water strider for low adhesion and low-energy dissipation. Langmuir 26(24):18926–37. https://doi.org/10.1021/la103442b
22. Das A, Sengupta S, Deka J et al (2018) Synthesis of fish scale and lotus leaf mimicking, stretchable and durable multilayers. J Mater Chem A 6:15993–16002. https://doi.org/10.1039/c8ta04984j
23. Zhang J, Wu L, Zhang Y, Wang A (2015) Mussel and fish scale-inspired underwater superoleophobic kapok membranes for continuous and simultaneous removal of insoluble oils and soluble dyes in water. J Mater Chem A 3:18475–18482. https://doi.org/10.1039/c5ta04839g
24. Sethi SK, Manik G, Sahoo SK (2019) Fundamentals of superhydrophobic surfaces. Elsevier Inc, Amsterdam
25. Bormashenko E, Gendelman O, Whyman G (2012) Superhydrophobicity of lotus leaves versus birds wings: different physical mechanisms leading to similar phenomena. Langmuir 28:14992–14997. https://doi.org/10.1021/la303340x
26. Kumar A, Kar S (2024) A study on functionalization process of silicon dioxide nanoparticles for hydrophobic coating applications. Surf Interface Anal. https://doi.org/10.1002/sia.7305
27. Jeevahan J, Chandrasekaran M, Britto Joseph G et al (2018) Superhydrophobic surfaces: a review on fundamentals, applications, and challenges. J Coatings Technol Res 15:231–250. https://doi.org/10.1007/s11998-017-0011-x
28. Ma M, Hill RM (2006) Superhydrophobic surfaces. Curr Opin Colloid Interface Sci 11:193–202. https://doi.org/10.1016/j.cocis.2006.06.002
29. Wang D, Sun Q, Hokkanen MJ et al (2020) Design of robust superhydrophobic surfaces. Nature 582:55–59. https://doi.org/10.1038/s41586-020-2331-8
30. Guo Z, Liu W, Su BL (2011) Superhydrophobic surfaces: from natural to biomimetic to functional. J Colloid Interface Sci 353:335–355. https://doi.org/10.1016/j.jcis.2010.08.047
31. Manoharan K, Bhattacharya S (2019) Superhydrophobic surfaces review: functional application, fabrication techniques and

limitations. J Micromanufacturing 2:59–78. https://doi.org/10.1177/2516598419836345
32. Wang C, Alpatova A, McPhedran KN, Gamal El-Din M (2015) Coagulation/flocculation process with polyaluminum chloride for the remediation of oil sands process-affected water: performance and mechanism study. J Environ Manage 160:254–262. https://doi.org/10.1016/j.jenvman.2015.06.025
33. Saththasivam J, Loganathan K, Sarp S (2016) An overview of oil-water separation using gas flotation systems. Chemosphere 144:671–680. https://doi.org/10.1016/j.chemosphere.2015.08.087
34. Tawalbeh M, Al Mojjly A, Al-Othman A, Hilal N (2018) Membrane separation as a pre-treatment process for oily saline water. Desalination 447:182–202. https://doi.org/10.1016/j.desal.2018.07.029
35. Yue X, Li J, Zhang T et al (2017) In situ one-step fabrication of durable superhydrophobic-superoleophilic cellulose/LDH membrane with hierarchical structure for efficiency oil/water separation. Chem Eng J 328:117–123. https://doi.org/10.1016/j.cej.2017.07.026
36. Huang L, Deng S, Guan J et al (2018) Development of a novel high-efficiency dynamic hydrocyclone for oil–water separation. Chem Eng Res Des 130:266–273. https://doi.org/10.1016/j.cherd.2017.12.030
37. Jamaly S, Giwa A, Hasan SW (2015) Recent improvements in oily wastewater treatment: progress, challenges, and future opportunities. J Environ Sci (China) 37:15–30. https://doi.org/10.1016/j.jes.2015.04.011
38. Fakhru'l-Razi A, Pendashteh A, Abdullah LC et al (2009) Review of technologies for oil and gas produced water treatment. J hazard mater 170(2–3):530–51. https://doi.org/10.1016/j.jhazmat.2009.05.044
39. Marmur A, Della VC, Siboni S et al (2017) Contact angles and wettability: towards common and accurate terminology. Surf Innov 5:3–8. https://doi.org/10.1680/jsuin.17.00002
40. Nakae H, Inui R, Hirata Y, Saito H (1998) Effects of surface roughness on wettability. Acta Mater 46:2313–2318. https://doi.org/10.1016/s1359-6454(98)80012-8
41. Song X, Qin Y, Ma H et al (2019) A new method to determine wettability of tight sandstone: water imbibition evaporation rate ratio measurements. Energy Fuels 33:1998–2007. https://doi.org/10.1021/acs.energyfuels.8b04184
42. Alghunaim A, Kirdponpattara S, Newby BMZ (2016) Techniques for determining contact angle and wettability of powders. Powder Technol 287:201–215. https://doi.org/10.1016/j.powtec.2015.10.002
43. Hebbar RS, Isloor AM, Ismail AF (2017) Contact Angle Measurements. Elsevier B.V, Amsterdam
44. Kwok DY, Neumann AW (1999) Contact angle measurement and contact angle interpretation. Adv Colloid Interface Sci 81:167–249
45. Comanns P (2018) Passive water collection with the integument mechanisms and their biomimetic potential. J Exp Biol 221(10):jeb153130
46. Baig U, Faizan M, Sajid M (2020) Multifunctional membranes with super-wetting characteristics for oil-water separation and removal of hazardous environmental pollutants from water: a review. Adv Colloid Interface Sci 285:102276. https://doi.org/10.1016/j.cis.2020.102276
47. Susana L, Campaci F, Santomaso AC (2012) Wettability of mineral and metallic powders: applicability and limitations of sessile drop method and Washburn's technique. Powder Technol 226:68–77. https://doi.org/10.1016/j.powtec.2012.04.016
48. Chau TT (2009) A review of techniques for measurement of contact angles and their applicability on mineral surfaces. Miner Eng 22:213–219. https://doi.org/10.1016/j.mineng.2008.07.009
49. Kumar A, Mishra V, Negi S, Kar S (2023) A systematic review on polymer-based superhydrophobic coating for preventing biofouling menace. J Coatings Technol Res. https://doi.org/10.1007/s11998-023-00773-8
50. Deng Y, Peng C, Dai M et al (2020) Recent development of super-wettable materials and their applications in oil-water separation. Elsevier Ltd, Amsterdam
51. Han Z, Mu Z, Yin W et al (2016) Biomimetic multifunctional surfaces inspired from animals. Adv Colloid Interface Sci 234:27–50. https://doi.org/10.1016/j.cis.2016.03.004
52. Yang J, Li HN, Chen ZX et al (2019) Janus membranes with controllable asymmetric configurations for highly efficient separation of oil-in-water emulsions. J Mater Chem A 7:7907–7917. https://doi.org/10.1039/C9TA00575G
53. Chen C, Weng D, Mahmood A et al (2019) Separation mechanism and construction of surfaces with special wettability for oil/water separation. ACS Appl Mater Interfaces 11:11006–11027. https://doi.org/10.1021/acsami.9b01293
54. Song B, Xu Q (2016) Highly hydrophobic and superoleophilic nanofibrous mats with controllable pore sizes for efficient oil/water separation. Langmuir 32:9960–9966. https://doi.org/10.1021/acs.langmuir.6b02500
55. Ohya H, Kim JJ, Chinen A et al (1998) Effects of pore size on separation mechanisms of microfiltration of oily water, using porous glass tubular membrane. J Memb Sci 145:1–14. https://doi.org/10.1016/S0376-7388(98)00067-2
56. Chen PC, Xu ZK (2013) Mineral-coated polymer membranes with superhydrophilicity and underwater superoleophobicity for effective oil/water separation. Sci Rep 3:1–6. https://doi.org/10.1038/srep02776
57. Solomon BR, Hyder MN, Varanasi KK (2014) Separating oil-water nanoemulsions using flux-enhanced hierarchical membranes. Sci Rep 4:1–6. https://doi.org/10.1038/srep05504
58. Chen Q, de Leon A, Advincula RC (2015) Inorganic–organic thiol–ene coated mesh for oil/water separation. ACS appl mater interfaces 7(33):18566–73
59. Xiong Y, Xu L, Nie K et al (2019) Green construction of an oil-water separator at room temperature and its promotion to an adsorption membrane. Langmuir 35:11071–11079. https://doi.org/10.1021/acs.langmuir.9b01480
60. Feng L, Zhang Z, Mai Z et al (2004) A super-hydrophobic and super-oleophilic coating mesh film for the separation of oil and water. Angew Chemie - Int Ed 43:2012–2014. https://doi.org/10.1002/anie.200353381
61. Qing W, Shi X, Deng Y et al (2017) Robust superhydrophobic-superoleophilic polytetrafluoroethylene nanofibrous membrane for oil/water separation. J Memb Sci 540:354–361. https://doi.org/10.1016/j.memsci.2017.06.060
62. Qin F, Yu Z, Fang X et al (2009) A novel composite coating mesh film for oil-water separation. Front Chem Eng China 3:112–118. https://doi.org/10.1007/s11705-009-0149-x
63. Khosravi M, Azizian S (2017) Preparation of superhydrophobic and superoleophilic nanostructured layer on steel mesh for oil-water separation. Sep Purif Technol 172:366–373. https://doi.org/10.1016/j.seppur.2016.08.035
64. Guo D, Chen J, Hou K et al (2018) A facile preparation of superhydrophobic halloysite-based meshes for efficient oil–water separation. Appl Clay Sci 156:195–201. https://doi.org/10.1016/j.clay.2018.01.034
65. Guo D, Hou K, Xu S et al (2018) Superhydrophobic–superoleophilic stainless steel meshes by spray-coating of a POSS hybrid acrylic polymer for oil–water separation. J Mater Sci 53:6403–6413. https://doi.org/10.1007/s10853-017-1542-3
66. Zhang Y, Wang X, Wang C et al (2018) Facile fabrication of zinc oxide coated superhydrophobic and superoleophilic meshes for

efficient oil/water separation. RSC Adv 8:35150–35156. https://doi.org/10.1039/c8ra06059b
67. Zhang Y, Wang H, Wang X et al (2021) An anti-oil-fouling and robust superhydrophilic $MnCo_2O_4$ coated stainless steel mesh for ultrafast oil/water mixtures separation. Sep Purif Technol 264:118435. https://doi.org/10.1016/j.seppur.2021.118435
68. Rahmatabadi D, Mohammadi B, Hashemi R, Shojaee T (2018) An experimental study of fracture toughness for nano/ultrafine grained Al5052/Cu multilayered composite processed by accumulative roll bonding. J Manuf Sci Eng 140(10):101001. https://doi.org/10.1115/1.4040542
69. Etemadi E, Rahmatabadi D, Hosseini SM (2020) Experimental investigation of spring-back phenomenon through an L-die bending process for multilayered sheets produced by the accumulative press bonding technique. Proc Inst Mech Eng, Part L: J Mater: Des Appl 234(12):1550–9. https://doi.org/10.1177/1464420720948888
70. Cao H, Gu W, Fu J et al (2017) Preparation of superhydrophobic/oleophilic copper mesh for oil-water separation. Appl Surf Sci 412:599–605. https://doi.org/10.1016/j.apsusc.2017.04.012
71. Liu Y, Zhang K, Yao W et al (2016) A facile electrodeposition process for the fabrication of superhydrophobic and superoleophilic copper mesh for efficient oil-water separation. Ind Eng Chem Res 55:2704–2712. https://doi.org/10.1021/acs.iecr.5b03503
72. Zhang F, Shi Z, Chen L et al (2017) Porous superhydrophobic and superoleophilic surfaces prepared by template assisted chemical vapor deposition. Surf Coatings Technol 315:385–390. https://doi.org/10.1016/j.surfcoat.2017.02.058
73. Khosravi M, Azizian S, Boukherroub R (2019) Efficient oil/water separation by superhydrophobic Cu_xS coated on copper mesh. Sep Purif Technol 215:573–581. https://doi.org/10.1016/j.seppur.2019.01.039
74. Luo ZY, Chen KX, Wang YQ et al (2016) Superhydrophilic nickel nanoparticles with core-shell structure to decorate copper mesh for efficient oil/water separation. J Phys Chem C 120:12685–12692. https://doi.org/10.1021/acs.jpcc.6b03940
75. You Q, Ran G, Wang C et al (2018) A novel superhydrophilic–underwater superoleophobic Zn-ZnO electrodeposited copper mesh for efficient oil/water separation. Sep Purif Technol 193:21–28. https://doi.org/10.1016/j.seppur.2017.10.055
76. Rahmatabadi D, Tayyebi M, Hashemi R (2018) Evaluation of microstructure and mechanical properties of multilayer Al5052–Cu composite produced by accmulative roll bonding. Powder Metall Metal Ceram 57:144–53. https://doi.org/10.1007/s11106-018-9962-4
77. Tayyebi M, Rahmatabadi D, Adhami M, Hashemi R (2019) Influence of ARB technique on the microstructural, mechanical and fracture properties of the multilayered Al1050/Al5052 composite reinforced. Integr Med Res 8:4287–4301. https://doi.org/10.1016/j.jmrt.2019.07.039
78. Mishra V, Negi S, Kar S et al (2022) Recent advances in fused deposition modeling fused deposition modeling based additive manufacturing of thermoplastic composite structures: a review. J Thermoplast Compos Mater. https://doi.org/10.1177/08927057221102857
79. Mishra V, Negi S, Kar S (2023) Additive manufacturing: an emerging tool to fabricate bioinspired structures. Lect Notes Mech Eng. https://doi.org/10.1007/978-981-19-3266-3_23
80. Qian X, Ostwal M, Asatekin A et al (2022) A critical review and commentary on recent progress of additive manufacturing and its impact on membrane technology. J Memb Sci 645:120041. https://doi.org/10.1016/j.memsci.2021.120041
81. Tijing LD, Dizon JRC, Ibrahim I et al (2020) 3D printing for membrane separation, desalination and water treatment. Appl Mater Today 18:100486. https://doi.org/10.1016/j.apmt.2019.100486
82. Lv J, Gong Z, He Z et al (2017) 3D printing of a mechanically durable superhydrophobic porous membrane for oil-water separation. J Mater Chem A 5:12435–12444. https://doi.org/10.1039/c7ta02202f
83. Guo Y, Luo B, Wang X et al (2022) Wettability control and oil/water separation performance of 3D-printed porous materials. J Appl Polym Sci 139:1–10. https://doi.org/10.1002/app.51570
84. Xing R, Huang R, Qi W et al (2018) Three-dimensionally printed bioinspired superhydrophobic PLA membrane for oil-water separation. AIChE J 64:3700–3708. https://doi.org/10.1002/aic.16347
85. Li X, Shan H, Zhang W, Li B (2020) 3D printed robust superhydrophilic and underwater superoleophobic composite membrane for high efficient oil/water separation. Sep Purif Technol 237:116324. https://doi.org/10.1016/j.seppur.2019.116324
86. Lee KM, Park H, Kim J, Chun DM (2019) Fabrication of a superhydrophobic surface using a fused deposition modeling (FDM) 3D printer with poly lactic acid (PLA) filament and dip coating with silica nanoparticles. Appl Surf Sci 467–468:979–991. https://doi.org/10.1016/j.apsusc.2018.10.205
87. Yang Y, Li X, Zheng X et al (2018) 3D-printed biomimetic superhydrophobic structure for microdroplet manipulation and oil/water separation. Adv Mater 30:1–11. https://doi.org/10.1002/adma.201704912
88. Yuan S, Strobbe D, Kruth JP et al (2017) Super-hydrophobic 3D printed polysulfone membranes with a switchable wettability by self-assembled candle soot for efficient gravity-driven oil/water separation. J Mater Chem A 5:25401–25409. https://doi.org/10.1039/c7ta08836a
89. Xing R, Yang B, Huang R et al (2019) Three-dimensionally printed bioinspired superhydrophobic packings for oil-in-water emulsion separation. Langmuir 35:12799–12806. https://doi.org/10.1021/acs.langmuir.9b02131
90. Zhai G, Qi L, He W et al (2021) Durable super-hydrophobic $PDMS@SiO_2@WS_2$ sponge for efficient oil/water separation in complex marine environment. Environ Pollut 269:116118. https://doi.org/10.1016/j.envpol.2020.116118

Publisher's Note Springer Nature remains neutral with regard to jurisdictional claims in published maps and institutional affiliations.